construction materials

MDPI

Article

Bio-Based Chitin for Cement Pastes: From Surface Interactions to Mechanical Performance

Khouloud Ben Chaabene [1,2,*], Geoffrey Promis [2] and Marzouk Lajili [1,*]

[1] EMIR Laboratory (Étude des Milieux Ionisés et Réactifs), University of Monastir, 15 Avenue Ibn Eljazzar IPEIM, Monastir 5019, Tunisia
[2] Innovative Technologies Laboratory (UR UPJV 3899), University of Picardie Jules Verne, Avenue des Facultés, Le Bailly, 80025 Amiens, France; geoffrey.promis@u-picardie.fr
* Correspondence: khouloud.benchaabene@fsm.rnu.tn (K.B.C.); marzouk.lajili@ipeim.rnu.tn (M.L.)

Abstract

Chitin, a bio-based polymer derived from crustacean shells, has attracted growing interest as a sustainable additive for cementitious materials due to its biodegradability and reactive hydroxyl and acetamide functional groups. In this study, chitin extracted from blue crab shells was incorporated into cement paste at 0, 1, 2, and 3 wt.% of cement to investigate its effects on mechanical performance, moisture sorption, and microstructural evolution. The extracted chitin was characterized by Fourier Transform Infrared Spectroscopy, X-ray Diffraction, Thermogravimetric Analysis, and Scanning Electron Microscopy. Cement pastes were evaluated using compressive strength testing, Dynamic Vapor Sorption (DVS), the Guggenheim–Anderson–de Boer (GAB) adsorption model, and SEM observations. The incorporation of 3 wt.% chitin increased the compressive strength by 56.8% compared with the reference paste. DVS and GAB analyses revealed enhanced water adsorption and an increase in accessible adsorption sites with increasing chitin content. SEM observations indicated a progressively denser and more homogeneous microstructure, accompanied by a reduction in visible porosity, as the chitin content increased. These findings suggest that chitin promotes favorable physicochemical interactions within the hydrated cement matrix, resulting in improved microstructural compactness and mechanical performance, highlighting its potential as a sustainable bio-based polymer for cement-based materials.

Keywords: chitin; bio-based polymer; cement paste; dynamic vapor sorption; GAB model; physicochemical interactions; mechanical performance

1. Introduction

The cement industry is a major contributor to global anthropogenic CO_2 emissions, making the reduction of its environmental footprint a major challenge for the construction sector. Among the most promising approaches is the incorporation of renewable bio-based materials and natural fibers of animal, plant, and mineral origin into cementitious materials, offering more sustainable alternatives that are receiving increasing attention in the construction industry [1–4]. Within this framework, biopolymers have attracted considerable interest as sustainable admixtures capable of modifying the performance of cementitious materials without necessarily replacing the cement binder [5]. Several classes of biopolymers have been investigated. For example, algae-derived biopolymers, including carrageenan, alginate, and ulvan, have been incorporated into cement-stabilized earth systems, where SEM observations revealed a denser C–S–H matrix, a refined interfacial

Check for updates

Received: 30 July 2026
Revised: 21 September 2026
Accepted: 23 September 2026
Published: 25 September 2026

Copyright: © 2026 by the authors. Licensee MDPI, Basel, Switzerland. This article is an open access article distributed under the terms and conditions of the Creative Commons Attribution (CC BY) license.

transition zone, and smaller portlandite crystals, resulting in enhanced mechanical performance and durability [6]. Likewise, cellulose nanocrystals have been incorporated into alkali-activated cementitious composites produced by 3D printing, improving the degree of hydration while reducing extrusion pressure by up to 35% [7]. Chitosan-based bio-inspired polymers have also been reported to enhance compressive and tensile strengths, reduce drying shrinkage, and improve the carbonation resistance of cement mortars [8]. Nevertheless, compared with conventional mineral and synthetic admixtures, the use of biopolymers in ordinary Portland cement-based materials remains relatively underexplored [9].

Among these bio-based materials, chitin—the second most abundant natural polysaccharide after cellulose—has emerged as a particularly attractive candidate. It is naturally synthesized by a wide variety of organisms, with an estimated annual biosynthesis of 10^{10}–10^{11} tons. However, only a small fraction, mainly originating from seafood-processing waste such as crustacean shells, is currently recovered and valorized, and its application in cementitious materials remains limited [10,11]. Owing to its biodegradability, biocompatibility, non-toxicity, and favorable mechanical properties, chitin has been extensively investigated for applications in water treatment, food packaging [12], biomedical engineering [13–16], and food preservation [17,18]. In addition, its chelating ability toward heavy metals and organic dyes has attracted considerable interest for wastewater treatment applications [19].

Recent studies have begun to demonstrate the potential of chitin and its derivatives as functional additives in cementitious materials. Haider et al. [20] investigated chitin nanocrystals (ChNC) and chitin nanofibers (ChNF) derived from shrimp-shell waste as additives in cement paste. At low dosages, these nanochitin forms modified the fresh and hardened behavior of the cementitious matrix, with delays in final setting time and improvements in mechanical performance; at an incorporation level of 0.05 wt.%, increases of approximately 40% in flexural strength and up to 12% in compressive strength were reported. In a complementary investigation on mortar, Haider et al. [21] showed that ChNC and ChNF influenced not only setting and mechanical properties but also late-age hydration. ChNF at 0.05 wt.% increased flexural strength and fracture energy by approximately 24% and 28%, respectively, while solid-state NMR indicated a more polymerized C–S–H structure and a higher degree of hydration. These findings suggest that particle morphology, aspect ratio, surface characteristics, and dosage strongly govern the interactions between chitin-based nanomaterials and the cement matrix.

Other studies, however, have shown that the beneficial effects of chitin-derived additives are not universal and depend strongly on their chemical form and concentration. Ortega et al. [22] investigated cement pastes containing 0.5–2.1 wt.% chitin after prolonged exposure to water and sulfate environments. By combining atomic force microscopy (AFM), Raman spectroscopy, Fourier transform infrared spectroscopy (FTIR), force spectroscopy, and compressive strength measurements, they established relationships between nanoscale elasticity and adhesion and the macroscopic mechanical behavior of the composites; nevertheless, increasing chitin content was associated with a reduction in mechanical performance. More recently, Baykara et al. [9] investigated shrimp-shell-derived chitosan particles at concentrations ranging from 0.05 to 2 wt.% in cement mortars. Their results indicated that chitosan affected the hydration process and produced only limited changes in mechanical performance, while the presence of chitosan particles appeared to slow cement hydration. Taken together, these studies demonstrate that the response of cementitious materials to chitin-derived additives is highly dependent on the form of the biopolymer (powder, nanocrystals, nanofibers, or chitosan), its dosage, particle characteristics, and its interaction with the hydration process.

Despite these recent advances, research on the direct incorporation of untreated chitin powder into Portland cement pastes remains limited. Most available studies have focused on highly processed forms such as chitin nanocrystals, chitin nanofibers, and chitosan [9,20,21]. Untreated chitin powder differs substantially from these materials in terms of particle dimensions, surface characteristics, and dispersion behavior, which may lead to different interactions with cement particles and hydration products. Moreover, the literature shows that chitin-derived additives may enhance or reduce mechanical performance depending on their form and concentration [9,20–22], highlighting the need to establish the behavior of non-nanoscale chitin powder separately. In particular, its influence on water-vapor sorption and microstructural development remains insufficiently documented, and the relationships between its physicochemical characteristics, interaction with the hydrated cement matrix, and resulting mechanical performance are not yet fully understood.

To better understand the physicochemical effects of chitin incorporation, complementary characterization techniques are required. FTIR spectroscopy provides information on the functional groups and chemical bonds involved in the chitin–cement system, while XRD enables the identification of crystalline phases and their evolution. TGA-DSC further provides information on mass-loss processes and thermal transformations associated with chitin and cement hydration products. The combined use of these techniques, together with microstructural and hygroscopic characterization, therefore provides a more comprehensive basis for interpreting the changes induced by chitin incorporation [20,23].

To address these knowledge gaps, the present study investigates the effect of crab-shell-derived chitin powder on the physicochemical, microstructural, hygroscopic, and mechanical properties of Portland cement pastes. Chitin was isolated from discarded crab shells collected from a seafood-processing plant in Bekalta (Monastir Governorate, Tunisia) and characterized before its incorporation into cement pastes at 0, 1, 2, and 3 wt.% relative to the cement mass. Particular attention was given to establishing relationships between water-vapor sorption behavior, microstructural modifications, and compressive strength to clarify the mechanisms governing the behavior of chitin-modified cement pastes. Beyond improving the understanding of non-nanoscale chitin in cementitious systems, this study contributes to the valorization of seafood-processing by-products as potential bio-based additives for construction materials.

2. Materials and Methods

2.1. Materials

This study investigates the chemical treatment of crab shell waste to extract chitin, a natural polymer, and explores its incorporation into cement to test its eventual effects on the properties and functionality of resulting material structures. The raw material used was the exoskeleton of blue crab "*P. segnis*", sourced from a Tunisian processing facility. All chemicals were analytical grade and procured from Sigma-Aldrich Chemical Co. (St. Louis, MO, USA). The Portland cement type used in this study was CEM II/A-LL 42.5, supplied by Cementir Holding (CPRO+, Cementir Holding N.V., Amsterdam, The Netherlands), and characterized by the chemical composition presented in Table 1. It served as the cement type for the preparation of all cement paste mixtures examined in this research.

Table 1. Cement chemical composition (%).

Fire Loss	SiO_2	Al_2O_3	Fe_2O_3	TiO_2	MnO	CaO	MgO	SO_3	K_2O	Na_2O	P_2O_5	S^-	Cl^-
6.8	18.2	4.1	2.1	0.2	0.1	62.2	1.8	2.9	0.83	0.11	0.2	0.03	0.06

2.2. Experimental Procedures

2.2.1. Chitin Extraction Process

The first step consisted of cleaning and drying the *P. segnis* crab shells. After cleaning, the shells were air-dried under sunlight for 24 h. Once dried, the shells were crushed using a planetary ball mill (RETSCH GmbH, Haan, Germany) operated at 200 rpm for 1 h. The resulting powder was then sieved through a 315 µm sieve to obtain particles with a controlled size before the subsequent chemical extraction steps.

The second phase focused on biomass demineralization. A 2 M hydrochloric acid (HCl) solution was used to remove the main inorganic component, calcium carbonate ($CaCO_3$), from the shells. The extraction was performed using a 1:10 (weight/volume) ratio of shell powder to HCl solution at 60 °C for 2 h under constant stirring at 350 rpm. After treatment, the material was filtered and thoroughly washed with distilled water until a neutral pH was reached. The material was then air-dried for 24 h at room temperature [24].

The subsequent deproteinization step involved treating the dried, demineralized material with 3 M sodium hydroxide (NaOH) solution at a 1:10 (weight/volume) ratio for 3 h at 80 °C under constant stirring. The resulting material was then filtered, thoroughly washed with distilled water, and dried under the same conditions as those used after demineralization. Finally, decolorization was performed by treating the isolated chitin from crab shells with a mild oxidizing solution composed of 0.1 M H_2O_2 and 10 mM HCl at a volume ratio of 9:1 [25]. After treatment, the product was thoroughly washed with distilled water and air-dried for 24 h at room temperature, yielding purified crab chitin.

2.2.2. Mix Proportions and Sample Preparation

The prepared chitin was incorporated into the cement at 1, 2, and 3 wt.% relative to the cement mass. The resulting cement–chitin composites were designated as CH0, CH1, CH2, and CH3, corresponding to chitin contents of 0, 1, 2, and 3 wt.%, respectively. Modified cement pastes were prepared using a water-to-cement ratio (w/c) of 0.45 with demineralized water. For each formulation, the required amount of chitin was incorporated into the cement before the addition of water to promote a homogeneous distribution of the chitin powder within the cement matrix. The mixtures were then mixed until a homogeneous cement paste was obtained.

All specimens were cast into cylindrical PVC molds with a diameter of 35 mm and a height of 70 mm, corresponding to a height-to-diameter ratio of 2:1. A thin layer of oil was applied to the inner surfaces of the molds before casting to facilitate demolding. After casting, the molds were placed on a vibrating table for 30 s to remove entrapped air and improve specimen compactness. After 24 h, the specimens were demolded and subsequently cured at 23 ± 2 °C and 50 ± 5% relative humidity for 28 days.

The overall chitin extraction procedure and sample preparation process are illustrated in Figure 1.

2.3. Method of Analysis

2.3.1. Characterization of the Chitin Powder

Fourier Transform Infrared Spectroscopy (FTIR) was performed in transmission mode using KBr pellets on a PerkinElmer infrared spectrometer (PerkinElmer Inc., Waltham, MA, USA). Chitin powder (2 mg) was homogeneously mixed with dry KBr (200 mg) and pressed into a pellet. The spectra were recorded in the range of 4000–450 cm^{-1} to identify the functional groups present in the chitin powder.

X-ray diffraction (XRD) analysis was conducted on a D4 Endeavor diffractometer (Bruker AXS GmbH, Karlsruhe, Germany) using Cu Kα radiation (λ = 1.54060 Å) to assess the crystallinity of the chitin powder. Approximately 200 mg of finely powdered chitin

sample was used for the analysis. The measurements were performed in locked-coupled geometry, with a step size of approximately 0.02° (2θ) and an acquisition time of 114.602 s per step.

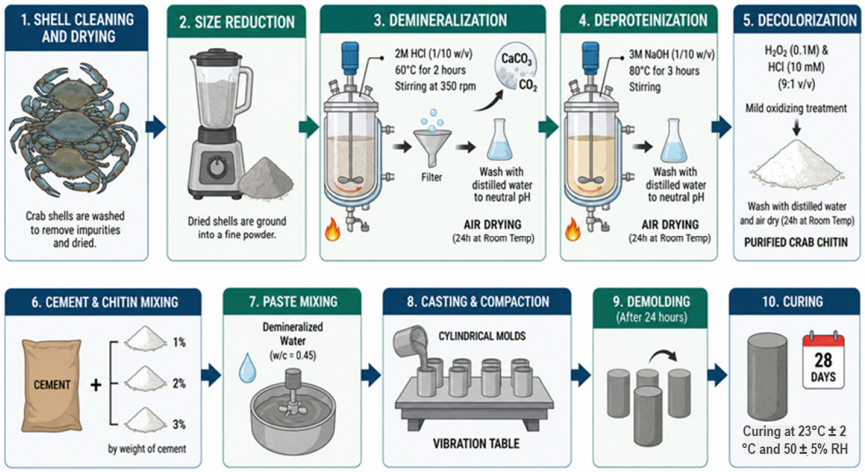


Figure 1. Schematic illustration of the extraction of chitin from blue crab shells and the preparation of cement paste samples.

Thermogravimetric analysis (TGA) was performed using a GP Concept T4/STA 449 F3 Jupiter simultaneous TGA-DSC system (NETZSCH-Gerätebau GmbH, Selb, Germany), coupled with a quadrupole mass spectrometer for the analysis of evolved gases. Approximately 20 mg of sample was placed in an alumina crucible and heated from 30 to 700 °C at a heating rate of 10 °C/min under an air atmosphere. The mass loss was continuously recorded as a function of temperature. Data acquisition and subsequent data processing were performed using NETZSCH Proteus software (version 8.0).

The surface morphology of the chitin powder was examined using a Scanning Electron Microscope (SEM). The analysis was performed on a Quanta 200 FEG SEM (FEI Company, Hillsboro, OR, USA). The sample was dried, mounted on adhesive tape, and coated with a 10 nm thick gold layer. Images were obtained under high-vacuum conditions using a secondary electron (SE) detector operated at an acceleration voltage of 10 kV.

Scanning Electron Microscopy was used to examine the microstructure and surface properties of the modified cement pastes, providing insights into their bonding behavior and morphological characteristics.

2.3.2. Characterization of the Chitin-Modified Cement Paste

The compressive strength test was performed in accordance with ASTM C39, adapted for small-scale cylindrical cement-based specimens [26]. Cylindrical specimens measuring 35 mm in diameter and 70 mm in height were tested after 28 days of curing using a Tinius Olsen H50KS universal testing machine (Tinius Olsen Testing Machine Company, Horsham, PA, USA) with a maximum load capacity of 50 kN. The tests were conducted under displacement control at a loading rate of 1 mm/min until failure. Before testing, the ends of the specimens were mechanically ground using a surface-grinding machine to obtain flat, parallel loading surfaces, thereby ensuring a more uniform stress distribution during loading and minimizing premature failure due to stress concentrations. Three specimens were tested for each formulation, and the mean compressive strength was calculated from the three measurements.

The water sorption behavior of the modified cement pastes was evaluated using a Dynamic Vapor Sorption (DVS) apparatus, ProUmid SPSx-1μ (ProUmid GmbH & Co. KG, Ulm, Germany). The measurements were performed with reference to ISO 12571:2021,

which specifies methods for determining the hygroscopic sorption properties of porous building materials [27]. The fully automated instrument operates according to the gravimetric principle and determines changes in sample mass under controlled relative humidity (RH) conditions at a constant temperature of 23 °C. Cubic specimens with dimensions of 1 cm^3 were placed in the climatic chamber of the instrument and exposed to different RH levels. The mass variations recorded at equilibrium during the sorption and desorption cycles were used to construct the corresponding isotherms. The instrument provides a mass resolution of 0.01 mg and a moisture content uncertainty of ±0.005%. Relative humidity is regulated with an accuracy of ±0.1% and an uncertainty of ±1% to ±1.5%. During testing, the RH was initially set at 0% and then increased stepwise from 0% to 90% in 10% increments. Each RH level was maintained until the sample mass reached equilibrium before proceeding to the next RH level. For each formulation, the absorption/desorption measurement was performed on a single specimen.

To quantitatively characterize the moisture adsorption behavior of the cement pastes, the experimental adsorption isotherms were fitted using the GAB model. Among the different mathematical models proposed for describing water vapor sorption in porous materials, the GAB model is one of the most widely accepted because it accounts for both monolayer adsorption and subsequent multilayer adsorption over a broad range of water activities. Unlike the Brunauer–Emmett–Teller (BET) model, whose applicability is generally restricted to water activities below approximately 0.5, the GAB model remains valid up to water activities close to 0.90, making it particularly suitable for cementitious materials, where significant moisture uptake occurs at high relative humidity. Consequently, the GAB model has been extensively applied to hardened cement pastes, concrete, bio-based construction materials, and natural polymers to investigate moisture storage mechanisms and to relate hygroscopic behavior to pore structure and internal surface characteristics [28].

The GAB equation is expressed as

$$\omega = \frac{\omega_m \, CK\phi}{(1 - K\phi)(1 - K\phi + CK\phi)} \quad (1)$$

where ω is the equilibrium moisture content (g/g), ω_m is the monolayer moisture content, ϕ is the relative humidity expressed as water activity (aw = RH/100), and C and K are dimensionless constants related to the sorption energy of the first adsorbed layer and the properties of multilayer water, respectively. The model parameters (ω_m, C, and K) were determined by nonlinear regression of the experimental adsorption data [29].

3. Results and Discussion

3.1. Characterization of Extracted Chitin

Figure 2 illustrates the chitin extracted from the crab shell, characterized using Fourier Transform Infrared Spectroscopy.

The FTIR spectra of the isolated chitin reveal distinctive features, including a prominent hydroxyl group peak at 3443 cm^{-1} and observed amide bands I, II, and III at 1658, 1558, and 1314 cm^{-1}, respectively. Additionally, NH stretching peaks appeared at 3107 cm^{-1} (Table 2). These observations are consistent with the findings of Kumari et al. [30], Liu et al. [31], and Jabeur et al. [32], confirming the successful extraction and preservation of the chitin structure.

The abundant hydroxyl (–OH) groups highlight the hydrophilic nature of chitin and promote hydrogen bonding with water molecules. Meanwhile, the amide functional groups provide additional polar sites capable of interacting with calcium ions and the surface of calcium silicate hydrate (C–S–H) through hydrogen bonding and electrostatic interactions. Owing to these functional groups, chitin is expected to exhibit good compatibility with the

hydrated cement matrix and may influence the organization of hydration products and the interfacial characteristics of the composite [19].

Figure 3 displays the diffractogram of the extracted chitin, obtained in the 2θ range of 10–70°. The XRD pattern shows four unique crystalline peaks at 13°, 19.6°, and 27°, validating the polymer's α-form [20]. Furthermore, it demonstrates several distinct peaks with a significant level of crystallinity.

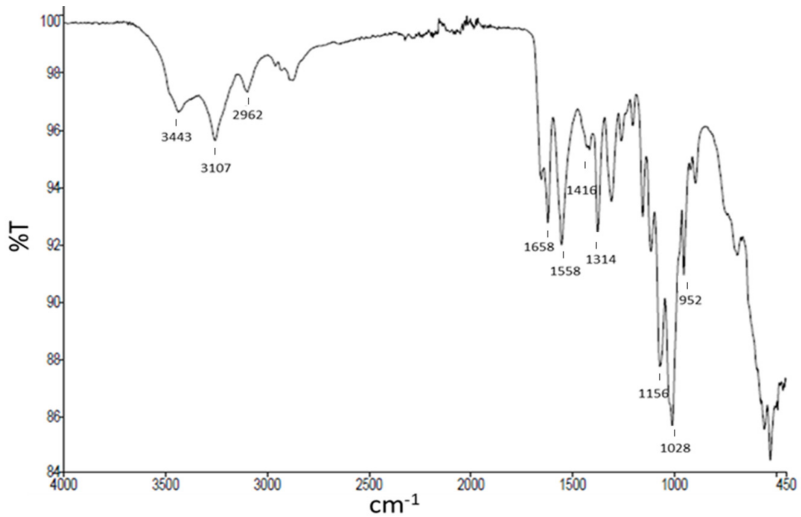


Figure 2. FTIR Spectra of the extracted chitin.

Table 2. Wavelengths of the bands obtained by the FT-IR of extracted chitin from crab shell powder.

Vibration Mode	Extracted Crab Chitin (cm^{-1})
OH stretching	3443
NH stretching	3107
Symmetric CH3 stretching and asymmetric CH2 stretching	2962
Amide I band	1658
Amide II band	1558
CH2 bending and CH3 deformation	1416
Amide III band and CH2 wagging	1314
Asymmetric bridge O2 stretching	1156
C-O stretching	1028
CH3 wagging along the chain	952

The crystallinity index (CrI) of the extracted chitin was calculated using the Segal method according to the following equation:

$$Cr(\%) = \frac{I_{110} - I_{am}}{I_{110}} \times 100 \quad (2)$$

where I_{110} is the maximum intensity of the crystalline region at 19.6°, and I_{am} is the maximum intensity of amorphous diffraction at 13°. The obtained crystallinity index was estimated at 81.3%, indicating a relatively high degree of crystallinity, comparable to values reported in the literature for α-chitin extracted from crustacean shells [33].

The crystallinity index achieved was calculated to be 81.3%, reflecting a notably high level of crystallinity, similar to those mentioned in the literature for α-chitin sourced from crustacean exoskeletons [33]. A crystallinity index of 81.3% indicates a significant amount of well-structured crystalline regions compared to the amorphous phase. A highly crystalline structure typically offers enhanced stiffness, better dimensional stability, and

increased resistance to thermal and chemical degradation compared to less crystalline chitin. These traits assist in maintaining the structural integrity of the biopolymer within alkaline surroundings, like cement pore solutions [9].

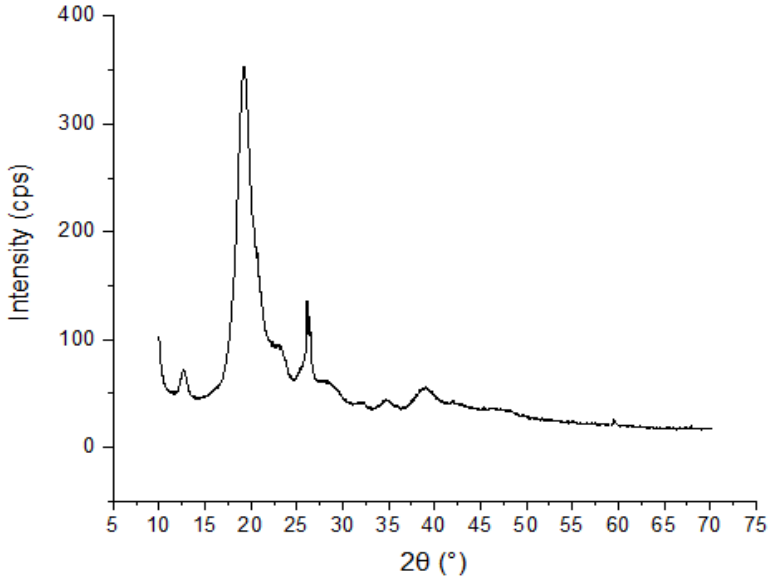


Figure 3. XRD patterns of chitin.

In cementitious materials, the relatively high crystallinity of chitin is also expected to enhance particle stability during hydration while maintaining its reinforcing role within the hydrated matrix. At the same time, the coexistence of crystalline domains and surface functional groups enables chitin to retain sufficient surface reactivity to interact with hydration products [34]. Therefore, the high crystallinity of the extracted chitin suggests that the biopolymer can preserve its structural integrity while remaining capable of interacting with the surrounding cementitious matrix. This combination of structural stability and surface functionality is advantageous for its use as a bio-based cement additive.

TGA was conducted to assess the correlation between sample mass loss and temperature treatment, and the results are shown in Figure 4.

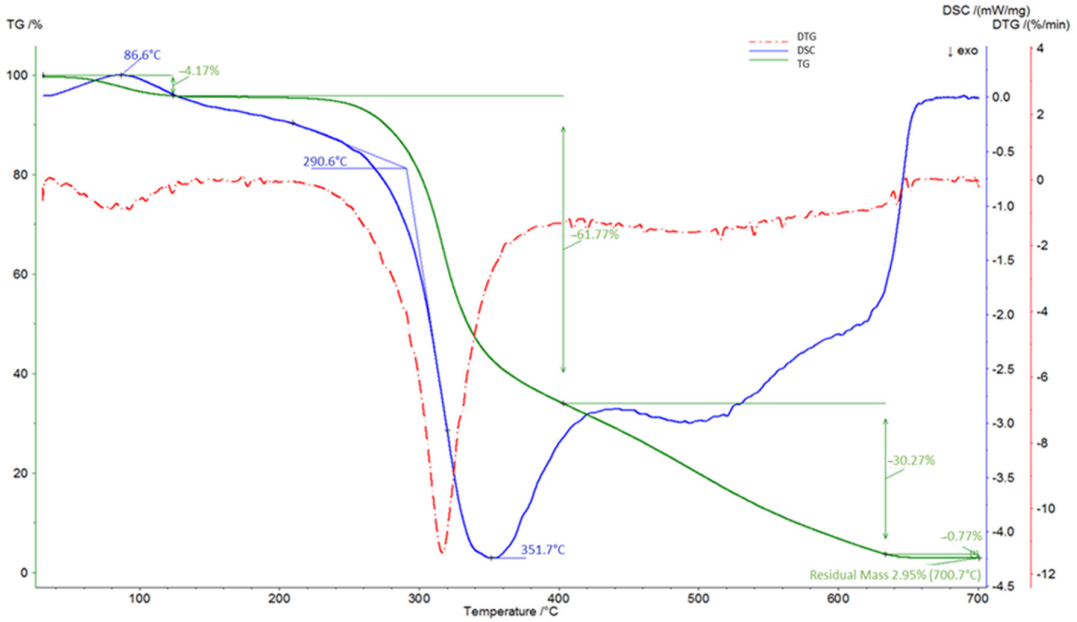


Figure 4. TG–DTG–DSC curves of extracted chitin.

The thermogram of chitin powder reveals a multi-stage decomposition process. Initially, degradation occurs between 50 °C and 150 °C, corresponding to the evaporation of physically adsorbed moisture, resulting in a mass loss of 4.17% [35]. This initial loss confirms the hygroscopic nature of chitin, attributable to the presence of abundant hydroxyl and amide functional groups.

The second degradation stage, spanning 150 to 400 °C, is the main decomposition region, accounting for 61.77% of the mass loss. An endothermic peak centered at 351.7 °C is observed and is attributed to the degradation of the chitin polymer chains through dehydration of saccharide rings, depolymerization, and decomposition of acetylated and deacetylated units [35]. The DTG curve shows a maximum degradation rate at 321.7 °C, indicating the temperature at which thermal decomposition proceeds most rapidly.

A third degradation stage occurs between 400 and 630 °C, with an additional mass loss of 30.27% and an exothermic peak at approximately 450 °C, which is commonly associated with the oxidation of carbonaceous residues formed during the previous decomposition stage. Finally, a residual mass of 0.77% persists at 700.7 °C, reflecting the inorganic ash content of the obtained chitin.

In general, the thermogravimetric analysis shows that chitin maintains thermal stability until around 250 °C, beyond which considerable degradation starts. This comparatively elevated thermal stability is primarily due to the structured molecular arrangement and wide hydrogen-bonding network typical of α-chitin. This stability benefits cementitious uses since the temperatures experienced during cement mixing, hydration, curing, and regular service conditions stay significantly lower than the threshold for thermal degradation. Consequently, the chitin particles are expected to preserve their structural integrity and surface functional groups throughout the hydration process, allowing them to maintain their potential interactions with the cement hydration products and the surrounding matrix.

SEM analysis of chitin is also presented, and the resulting scans are depicted in Figure 5.

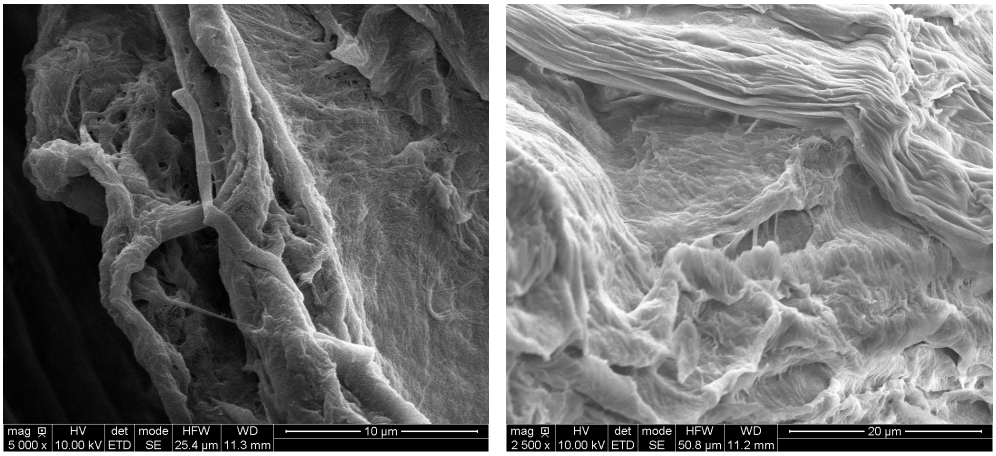


Figure 5. SEM images of chitin (×5000 and ×2500).

The scan suggests that the chitin surface exhibits a rough, porous structure. Further examination revealed the presence of porous and fibril structures within the biopolymer [24]. The observation of a continuous and uniform porous structure indicates an interaction feature among the chitin molecules.

3.2. Performance of Chitin-Modified Cement Paste

3.2.1. Compressive Strength

Figure 6 presents the results of the compressive strength test for the reference CH0 and mixes prepared with chitin–cement at various replacement percentages. Three cylindrical samples were tested for each percentage. Mechanical testing was conducted on composites cured for 28 days. Notably, the control samples consisting solely of cement exhibited considerably lower strength, averaging 17.6 MPa. In contrast, compressive strength increased as the chitin percentage rose from 1% to 3%. More precisely, at a chitin concentration of 3%, the strength increased by 56.8% compared to the control samples, reaching 27.6 MPa.

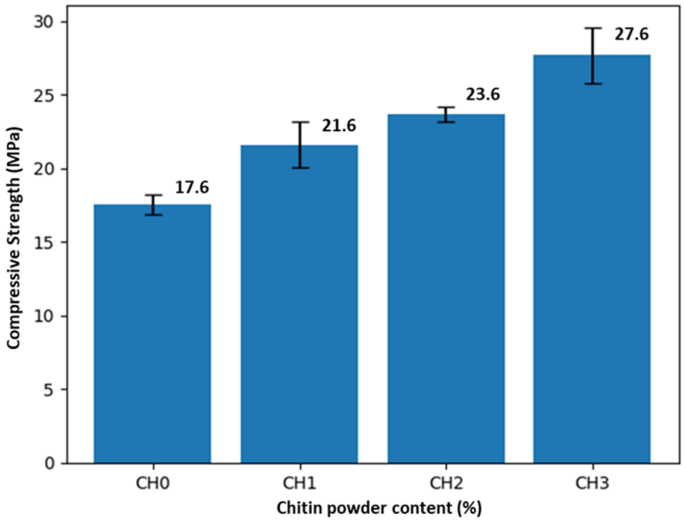


Figure 6. Compressive strength test of Chitin–Cement composites.

The improvement in compressive strength may be attributed to the ability of chitin particles to modify the cement matrix through void filling and pore refinement. Their surface characteristics may also provide additional nucleation sites for hydration products, promoting C–S–H formation and contributing to a denser and more homogeneous microstructure [20,36]. Similar mechanisms have been reported for finely divided mineral and bio-based additives, where particle packing, pore refinement, and particle–matrix interactions contribute to mechanical performance [37].

The present results are consistent with previous studies showing that chitin-derived additives can modify the mechanical behavior of cementitious materials, although the magnitude and direction of the effect depend strongly on their form and dosage. In the present study, the compressive strength increased from 17.6 MPa for CH0 to 27.6 MPa for CH3, corresponding to an improvement of 56.8% at 28 days. Haider et al. [20] reported an increase of up to approximately 12% in 28-day compressive strength using only 0.05 wt.% ChNC or ChNF. In contrast, Ortega et al. [22] observed a progressive decrease in mechanical performance with increasing chitin content (0.5–2.1 wt.%), while Baykara et al. [9] reported that the effect of chitosan on mortar strength varied with dosage and was accompanied by changes in cement hydration. These differences highlight the importance of particle size, morphology, chemical form, concentration, and dispersion in governing the interaction of chitin-derived materials with the cement matrix.

Compared with conventional mineral fillers such as limestone powder, fly ash, silica fume, or metakaolin, chitin is an organic biopolymer whose hydroxyl and acetamide groups and affinity for water may introduce additional interactions with the hydrated cement matrix. Therefore, its contribution cannot be explained solely by a physical filler effect. Within the range investigated here, strength increased continuously up to 3 wt.%

chitin; however, this value should be considered the highest dosage tested rather than an optimum content. Further investigation at higher dosages is required to determine whether a threshold exists beyond which the beneficial effect on mechanical performance decreases.

To further elucidate the mechanisms underlying the observed improvement in compressive strength, the moisture sorption behavior and microstructural evolution of the cement pastes were subsequently investigated.

3.2.2. Water Vapor Sorption Behavior

To investigate the influence of chitin incorporation on the hygroscopic behavior of cement paste, water vapor sorption isotherms were measured at 23 °C using the Dynamic Vapor Sorption (DVS) technique. Figure 7 presents the experimental water vapor adsorption–desorption isotherms of the reference paste (CH0) and the chitin-modified cement pastes (CH1, CH2, and CH3).

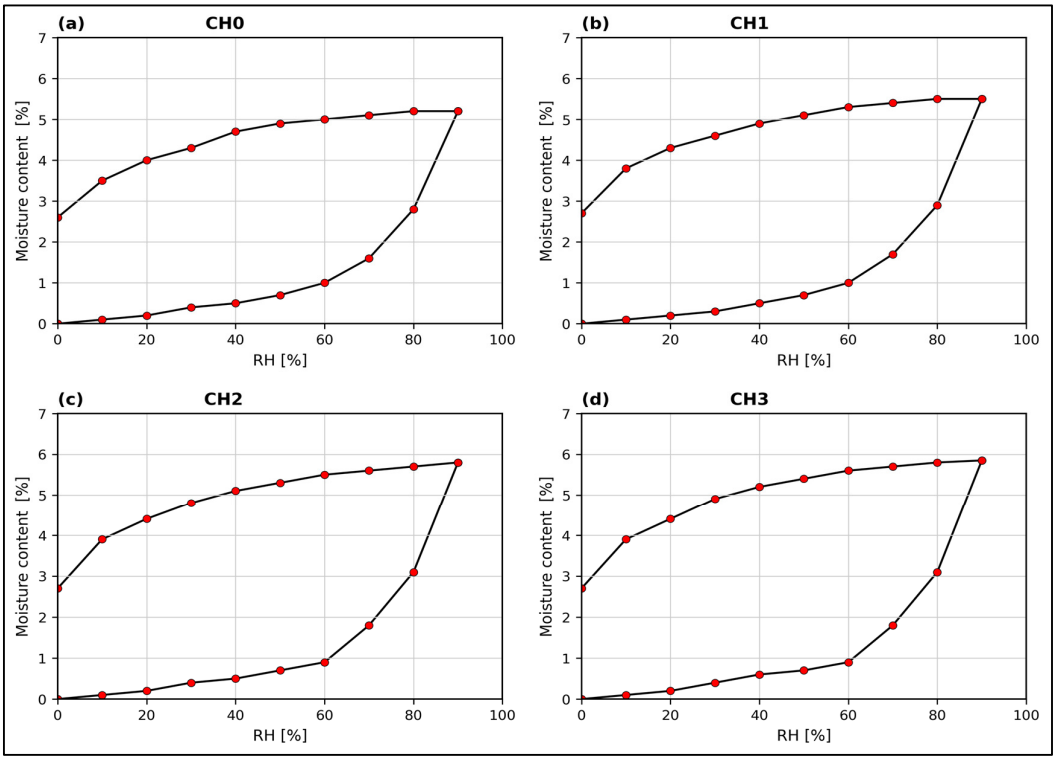


Figure 7. Sorption isotherm at 23 °C for biocomposite samples with different chitin contents: (**a**) CH0, (**b**) CH1, (**c**) CH3, and (**d**) CH4.

All formulations exhibited a typical sigmoidal adsorption–desorption isotherm, characteristic of hardened cementitious materials. According to the IUPAC classification, this behavior corresponds to a Type II isotherm, which is generally associated with multilayer adsorption occurring on heterogeneous porous solids. Such behavior has been widely reported for hydrated cement pastes and reflects the progressive filling of the pore network as the relative humidity increases [38].

Compared with the reference paste (CH0), the chitin-containing pastes showed slightly higher equilibrium moisture contents, with the differences becoming more pronounced at high RH. At 90% RH, the observed equilibrium moisture content was approximately 5.2%, 11.3%, and 12.0% higher than that of CH0 for CH1, CH2, and CH3, respectively. Similar differences of 5.4%, 13.5%, and 12.8% were observed at 80% RH. These observations suggest that chitin incorporation may contribute to increased moisture uptake while preserving the overall shape of the sorption isotherm.

The higher moisture uptake may be related to chitin slightly modifying the internal microstructure of the hydrated cement paste. Besides the intrinsic hydrophilicity of chitin, resulting from its hydroxyl and acetamide functional groups, the increase in equilibrium moisture content may also be associated with changes in the accessible internal surface area and the interfacial regions between chitin particles and cement hydration products [39]. These microstructural features could provide additional adsorption sites for water molecules, particularly at high relative humidity, where multilayer adsorption and capillary condensation become predominant.

The similar overall shapes of the adsorption–desorption isotherms and hysteresis loops suggest that the incorporation of up to 3 wt.% chitin preserves the characteristic sorption behavior of hydrated cement paste. The observed differences may therefore be associated primarily with variations in accessible adsorption sites rather than a fundamental change in the sorption mechanism.

To quantitatively describe these adsorption phenomena and further examine the influence of chitin on the water sorption characteristics of the composites, the experimental adsorption isotherms were fitted using the Guggenheim–Anderson–de Boer (GAB) model.

3.2.3. GAB Model Analysis

Figure 8 compares the experimental adsorption isotherms with the corresponding GAB fittings for all investigated formulations. The fitted curves closely reflect the experimental data across the full range of water activity examined, suggesting that the GAB model successfully represents the adsorption characteristics of both the reference paste and the chitin-modified composites. The determination coefficients ($R2 > 0.98$) validate the strong correlation between the experimental results and the model forecasts, indicating that the adsorption process is primarily influenced by the mechanisms included in the GAB formulation, specifically monolayer adsorption succeeded by multilayer adsorption.

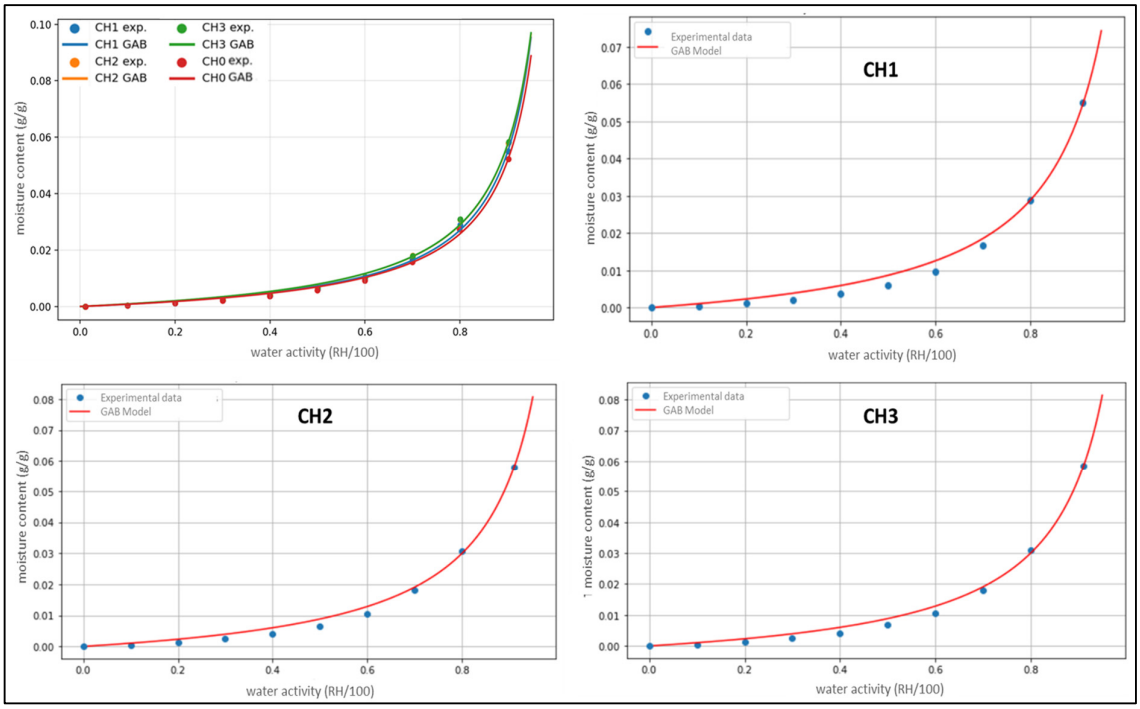


Figure 8. Comparison of experimental data with the adsorption curves fitted by the GAB model.

The correlation between the experimental data and the fitted curves is especially strong in the low and intermediate water activity ranges, where adsorption primarily happens on the internal surface of the C–S–H gel via the sequential creation of molecular water layers.

At higher water activities (>0.75), the model also reproduces the sharp increase in equilibrium moisture content associated with capillary condensation within the finest accessible pores. The ability of the GAB model to accurately describe this transition confirms that the pore structure of the investigated cement pastes remains dominated by gel pores and fine capillary pores, which are responsible for the rapid increase in moisture storage at high relative humidity [40].

Although the four adsorption curves exhibit very similar shapes, a slight upward shift is observed as chitin content increases, particularly for CH2 and CH3. This behavior indicates that chitin does not modify the fundamental adsorption mechanism but rather increases the equilibrium moisture adsorption capacity of the cement paste. Such an increase can be attributed to two complementary effects.

First, chitin is an intrinsically hydrophilic biopolymer containing hydroxyl and acetamide functional groups that can form hydrogen bonds with water molecules, thereby creating additional adsorption sites. Second, the incorporation of chitin slightly increases the accessible internal surface area and the interfacial regions between the biopolymer particles and the hydrated cement matrix, allowing a greater amount of water vapor to be retained at equilibrium [41]. This interpretation is consistent with the experimental DVS isotherms, which showed increases in equilibrium moisture content of approximately 5.2%, 11.3%, and 12.0% at 90% RH for CH1, CH2, and CH3, respectively, compared with the reference paste.

The GAB fitting, therefore, provides quantitative evidence that the incorporation of chitin mainly affects the adsorption capacity of the cement paste rather than the adsorption mechanism itself. The nearly parallel evolution of the four fitted curves suggests that the hydration products remain the dominant adsorption phase, while chitin contributes additional hydrophilic adsorption sites without significantly modifying the overall pore network. Similar behavior has been reported for cementitious composites incorporating bio-based polymers, where the increase in hygroscopicity was primarily attributed to the intrinsic hydrophilicity of the biopolymer and to slight modifications of the accessible pore structure rather than to major changes in total porosity [42].

The evolution of the GAB parameters presented in Table 3 further supports this interpretation. In particular, the progressive increase in the monolayer moisture content (ω_m) with increasing chitin dosage suggests an increase in the number of energetically favorable primary adsorption sites, thereby enhancing the hygroscopic capacity of the chitin-modified cement paste.

Table 3. Fitting parameters of the GAB model for adsorption isotherms.

Material	Phase	ω_m (g/g)	C	K	R^2
CH0	Adsorption	0.00734	248.0	0.9723	0.9965
CH1	Adsorption	0.00763	241.5	0.928	0.9894
CH2	Adsorption	0.00840	194.6	0.937	0.9936
CH3	Adsorption	0.00841	174.4	0.938	0.9938

Consequently, the observed increase in moisture uptake is mainly associated with the hydrophilic character of chitin and the increase in accessible adsorption sites rather than with a fundamental modification of the pore structure.

3.2.4. Proposed Physicochemical Interaction Mechanism Between Chitin and Cement Hydration Products

Figure 9 illustrates the proposed physicochemical interaction mechanism between chitin particles and the hydrated cement matrix. This mechanism is established based on the chemical characterization of the extracted chitin, the experimental results obtained in the present study, and previous investigations on the interactions between polysaccharides and cementitious materials. Although these interactions were not directly characterized at the molecular scale, they provide a consistent framework for interpreting the improvements observed in compressive strength, moisture sorption behavior, and microstructural evolution.

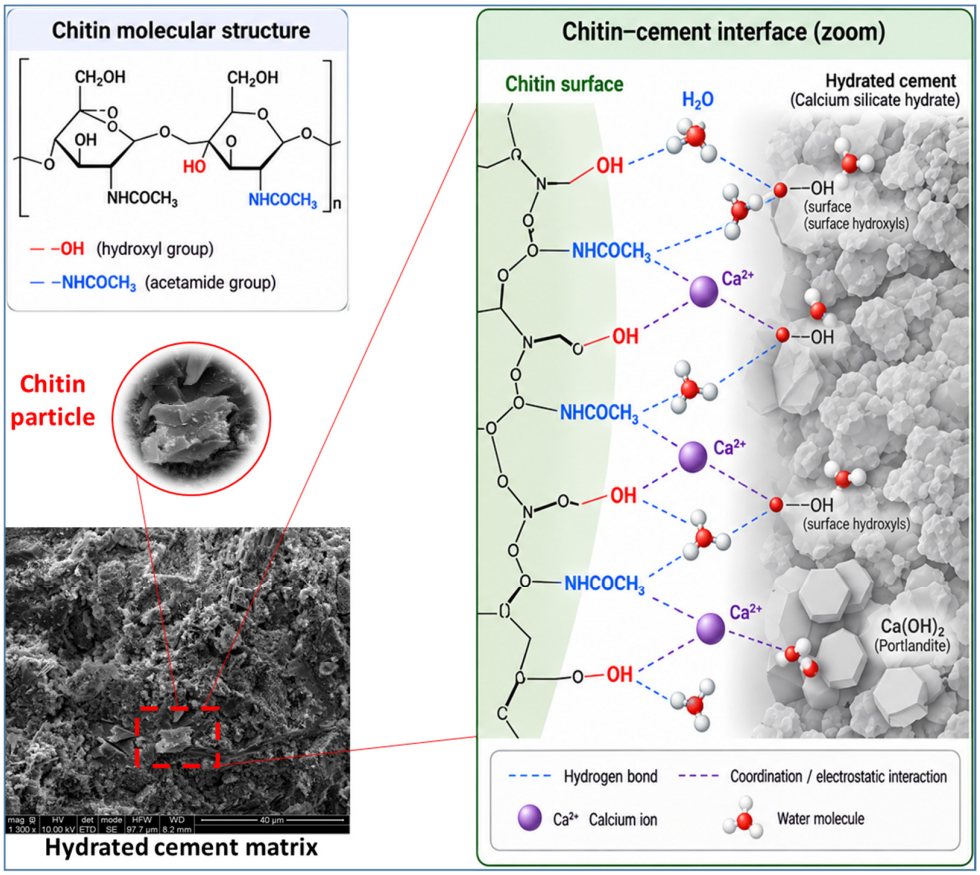


Figure 9. Physicochemical interactions between chitin particles and hydrated cement phases.

FTIR analysis indicates that the extracted chitin is rich in hydroxyl (–OH) and acetamide (–$NHCOCH_3$) functional groups scattered throughout its polymeric backbone. These polar groups give the biopolymer a strong hydrophilic nature and create chemically active sites that engage with both water molecules and the products of cement hydration. Hydroxyl and acetamide groups create hydrogen bonds with water molecules, resulting in tightly bound water layers and, as relative humidity rises, multilayer adsorption. This adsorption process has been widely documented for chitin and chitosan, illustrating their strong attraction to water vapor, which is closely linked to the existence of these functional groups [39,43].

In the process of cement hydration, the dissolution of alite and belite phases results in the release of calcium ions (Ca^{2+}), hydroxyl ions (OH^{-}), and silicate species, which causes the formation of calcium silicate hydrate (C–S–H) gel and portlandite ($Ca(OH)_2$) [44,45]. In such strongly alkaline environments, the hydroxyl and acetamide group oxygen atoms may engage with calcium ions via coordination and electrostatic forces, while hydrogen bonds could concurrently develop between the functional groups of chitin and the hy-

droxylated surfaces of C–S–H. These surface interactions are anticipated to enhance the compatibility of chitin particles with the adjacent cement matrix by facilitating improved particle–matrix adhesion.

Furthermore, the adsorption of calcium ions and hydrated silicate species on the chitin surface may create preferential sites for the heterogeneous nucleation of C–S–H. Although chitin does not directly participate in hydration reactions, its functionalized surface may facilitate the local precipitation and growth of hydration products, resulting in a more homogeneous distribution of C–S–H around the biopolymer particles. Similar nucleation mechanisms have been reported for finely dispersed bio-based nanomaterials and polysaccharides incorporated into cementitious systems, where they contribute to matrix densification and improved mechanical performance [20,45].

The combined effects of hydrogen bonding, calcium coordination, and preferential nucleation of hydration products are therefore proposed to explain the behavior of the chitin-modified cement pastes. These interactions may increase the number of hydrophilic adsorption sites, modify the moisture transport pathways within the pore network, and enhance the continuity of the hydrated matrix. Consequently, the proposed mechanism provides a plausible explanation for the higher equilibrium moisture contents obtained from the DVS measurements, the evolution of the GAB parameters, and the progressive increase in compressive strength observed with increasing chitin content.

3.2.5. Microstructural Analysis

To better understand the mechanisms responsible for the improvement in compressive strength and the slight changes in moisture sorption behavior, Figure 10 compares the SEM micrographs of the reference cement paste (CH0) and the paste containing 3 wt.% chitin (CH3) after 28 days of curing.

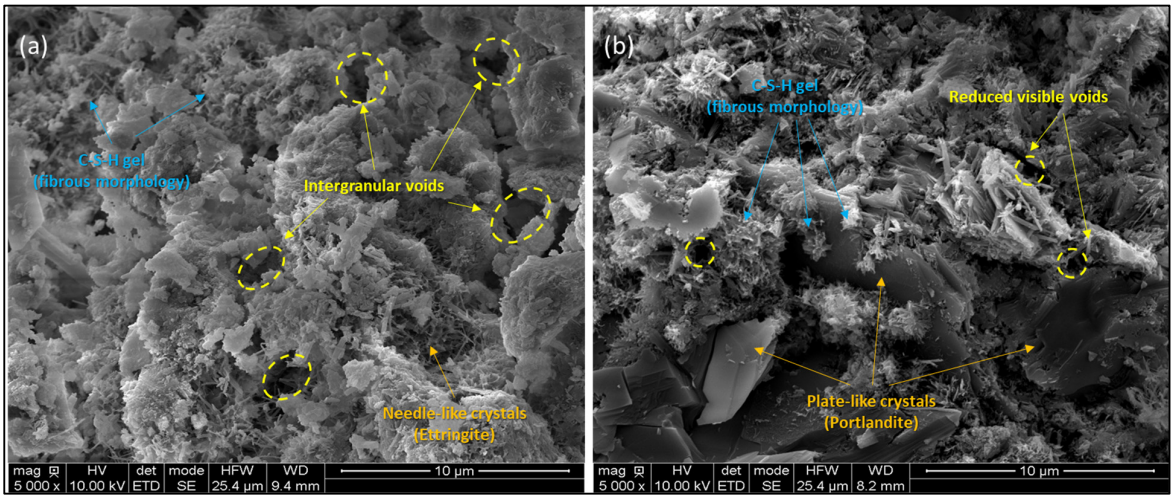


Figure 10. SEM micrographs of cement paste (×5000): (**a**) CH0 and (**b**) CH3.

The reference paste (CH0) displays a relatively heterogeneous microstructure, dominated by fibrous hydration products interspersed with numerous intergranular voids, reflecting a loosely packed and poorly connected hydrated matrix. By contrast, the CH3 specimen exhibits a markedly denser and more homogeneous microstructure, with a visible reduction in porosity and a continuous, well-interconnected network of hydration products. Plate-like crystals consistent with portlandite are embedded within the matrix, while the fibrous C–S–H morphology remains fully developed, indicating that hydration proceeds normally in the presence of chitin. Taken together, these features suggest that chitin pro-

motes a densification and refinement of the microstructure rather than the formation of additional or alternative hydration phases.

This microstructural refinement is consistent with the DVS and GAB results, which showed increased moisture adsorption and a greater number of accessible sorption sites as chitin content increased. Rather than resulting from higher pore volume, this enhanced water uptake is more plausibly explained by the hydrophilic hydroxyl and acetamide groups exposed on the chitin surface, which introduce additional sorption sites without compromising matrix compactness—a behavior previously reported for other biopolymers incorporated in cementitious systems [20,46]. Furthermore, the denser, more continuous hydrated matrix observed in CH3 correlates well with the substantial gain in compressive strength, reinforcing the proposed mechanism whereby favorable physicochemical interactions between chitin and the hydrating cement phases enhance matrix compactness and improve stress transfer throughout the paste. Similar relationships between matrix densification, pore refinement and mechanical performance have been extensively reported for cement-based composites [47].

4. Conclusions

This study investigated the potential of chitin extracted from blue crab shells as a sustainable bio-based additive for cement paste. FTIR and XRD analyses confirmed the characteristic structure of α-chitin, while thermal analysis demonstrated its thermal behavior and stability under the investigated conditions.

Chitin incorporation influenced the mechanical, hygroscopic, and microstructural behavior of the cement pastes. Among the investigated formulations, the paste containing 3 wt.% chitin exhibited the highest compressive strength, reaching a 56.8% increase compared with the reference paste. DVS measurements showed higher equilibrium moisture contents in the chitin-containing pastes, particularly at high relative humidity, while GAB modeling suggested changes in the accessible adsorption sites associated with chitin incorporation. SEM observations also showed a denser and more homogeneous microstructure with increasing chitin content, characterized by fewer visible intergranular voids and improved continuity of the hydrated matrix.

The combined findings suggest that the observed behavior may result from the contribution of chitin as a fine particulate additive together with interactions between its hydrophilic functional groups and the hydrated cement matrix. These effects may influence the interfacial environment, moisture adsorption, and microstructural organization, thereby contributing to the improved mechanical performance observed in the investigated formulations.

Overall, crab shell-derived chitin shows potential as a bio-based additive for cementitious materials while providing a valorization pathway for seafood waste within a circular economy framework. The present findings provide a basis for further investigation of chitin-modified cementitious materials, particularly regarding hydration kinetics, moisture transport, durability, and long-term performance. Future studies should also include replicate sorption measurements and extend the investigation to mortar and concrete to assess the reproducibility and practical applicability of the observed trends.

5. Perspectives

Future research should extend this approach to mortar and concrete and evaluate the influence of chitin on transport properties, shrinkage, durability, and long-term mechanical performance. Isothermal calorimetry could be used to investigate the effect of chitin on cement hydration kinetics and heat evolution. In addition, measuring the vapor sorption isotherms of pure chitin at mass fractions equivalent to 1, 2, and 3 wt.% would help

distinguish the intrinsic hygroscopic contribution of chitin from its effect on the cement matrix. SEM observations at early hydration ages (e.g., 1, 3, and 7 days) could further clarify the evolution of the microstructure and hydration products. Finally, optimization of chitin extraction and its large-scale valorization from seafood waste should be investigated to support potential industrial implementation.

Author Contributions: K.B.C.: Writing—original draft, methodology, validation, investigation, conceptualization, visualization. G.P.: Writing—review and editing, supervision, resources, funding acquisition. M.L.: Writing—review and editing, supervision, project administration. All authors have read and agreed to the published version of the manuscript.

Funding: This research received no external funding.

Data Availability Statement: The original contributions presented in this study are included in the article. Further inquiries can be directed to the corresponding authors.

Acknowledgments: The authors acknowledge the support provided for this work by the Laboratory of Innovative Technologies (LTI) at the University of Picardie Jules Verne. The authors would like to express their gratitude to Hatem Majdoub from the Faculty of Sciences of Monastir for providing them with the necessary chemical equipment and materials to prepare the samples and extract the chitin. The authors would like to express their gratitude to Arash Jamali, for his invaluable support and knowledge in obtaining the SEM images employed in this study.

Conflicts of Interest: The authors declare no conflicts of interest.

Abbreviations

The following abbreviations are used in this manuscript:

CH0	Paste containing 0 wt.% chitin
CH1	Paste containing 1 wt.% chitin
CH2	Paste containing 2 wt.% chitin
CH3	Paste containing 3 wt.% chitin

References

1. Martínez-García, C.; González-Fonteboa, B.; Martínez-Abella, F.; Carro-López, D. Performance of mussel shell as aggregate in plain concrete. *Constr. Build. Mater.* **2017**, *139*, 570–583. [CrossRef]
2. Onuaguluchi, O.; Banthia, N. Plant-based natural fiber reinforced cement composites: A review. *Cem. Concr. Compos.* **2016**, *68*, 96–108. [CrossRef]
3. Du, H.; Pang, S.D. Value-added utilization of marine clay as cement replacement for sustainable concrete production. *J. Clean. Prod.* **2018**, *198*, 867–873. [CrossRef]
4. Frías, M.; Savastano, H.; Villar, E.; Sánchez de Rojas, M.I.; Santos, S. Characterization and properties of blended cement matrices containing activated bamboo leaf wastes. *Cem. Concr. Compos.* **2012**, *34*, 1019–1023. [CrossRef]
5. Vignesh, J.; Ramesh, B.; Xavier, J.R. A Review of Recent Trends in Sustainable Biopolymer-Integrated Concrete and Its Impact on Mechanical Performance and Structural Reliability. *Int. J. Biol. Macromol.* **2025**, *321*, 146408. [CrossRef]
6. Kohandelnia, M.; Hayek, M.; Bouarab, K.; Yahia, A. New Perspectives into the Rheology of Earth Suspensions Modified with Algae-Derived Biopolymers. *Constr. Build. Mater.* **2025**, *503*, 144523. [CrossRef]
7. Al Fahim, A.; Admassu, N.; Dailey, G.; Moradllo, M.K. Application of Cellulose Nanocrystals in 3D Printed Alkali-Activated Cementitious Composites. *J. Build. Eng.* **2024**, *82*, 108380. [CrossRef]
8. Choi, S.J.; Bae, S.H.; Lee, J.I.; Bang, E.J.; Choi, H.Y.; Ko, H.M. Effect of Bio-Inspired Polymer Types on Engineering Characteristics of Cement Composites. *Polymers* **2022**, *14*, 1808. [CrossRef]
9. Baykara, H.; Riofrio, A.; Garcia-Troncoso, N.; Cornejo, M.; Tello-Ayala, K.; Flores Rada, J.; Caceres, J. Chitosan-Cement Composite Mortars: Exploring Interactions, Structural Evolution, Environmental Footprint and Mechanical Performance. *ACS Omega* **2024**, *9*, 24978–24986. [CrossRef]
10. Kozma, M.; Acharya, B.; Bissessur, R. Chitin, chitosan, and nanochitin: Extraction, synthesis, and applications. *Polymers* **2022**, *14*, 3989. [CrossRef]

11. El Knidri, H.; Belaabed, R.; Addaou, A.; Laajeb, A.; Lahsini, A. Extraction, chemical modification, and characterization of chitin and chitosan. *Int. J. Biol. Macromol.* **2018**, *120*, 1181–1189. [CrossRef]
12. Fernandez, J.G.; Ingber, D.E. Manufacturing of large-scale functional objects using biodegradable chitosan bioplastic. *Macromol. Mater. Eng.* **2014**, *299*, 932–938. [CrossRef]
13. Berezina, N. Production and application of chitin. *Phys. Sci. Rev.* **2016**, *1*, 20160048. [CrossRef]
14. Khor, E. *Chitin: Fulfilling a Biomaterials Promise*, 2nd ed.; Elsevier: Oxford, UK, 2014.
15. Singh, R.; Shitiz, K.; Singh, A. Chitin and chitosan: Biopolymers for wound management. *Int. Wound J.* **2017**, *14*, 1276–1289. [CrossRef]
16. Piekarska, K.; Sikora, M.; Owczarek, M.; Jóźwik-Pruska, J.; Wiśniewska-Wrona, M. Chitin and chitosan as polymers of the future—Obtaining, modification, life cycle assessment and main directions of application. *Polymers* **2023**, *15*, 793. [CrossRef]
17. Fatima, M.; Mir, S.; Ali, M.; Hassan, S.; Khan, Z.U.H.; Waqar, K. Synthesis and applications of chitosan derivatives in food preservation: A review. *Eur. Polym. J.* **2024**, *216*, 113242. [CrossRef]
18. Olivia, M.; Jingga, H.; Toni, N.; Wibisono, G. Biopolymers to improve physical properties and leaching characteristics of mortar and concrete: A review. *IOP Conf. Ser. Mater. Sci. Eng.* **2018**, *345*, 012028. [CrossRef]
19. Peter, S.; Lyczko, N.; Gopakumar, D.; Maria, H.J.; Nzihou, A.; Thomas, S. Chitin and chitosan based composites for energy and environmental applications: A review. *Waste Biomass Valorization* **2021**, *12*, 4777–4804. [CrossRef]
20. Haider, M.M.; Jian, G.; Zhong, T.; Li, H.; Fernandez, C.A.; Fifield, L.S.; Wolcott, M.; Nassiri, S. Insights into Setting Time, Rheological and Mechanical Properties of Chitin Nanocrystals- and Chitin Nanofibers-Cement Paste. *Cem. Concr. Compos.* **2022**, *132*, 104623. [CrossRef]
21. Haider, M.M.; Jian, G.; Li, H.; Miller, Q.R.S.; Wolcott, M.; Fernandez, C.; Nassiri, S. Impact of chitin nanofibers and nanocrystals from waste shrimp shells on mechanical properties, setting time, and late-age hydration of mortar. *Sci. Rep.* **2022**, *12*, 20539. [CrossRef]
22. Ortega, E.; Rodríguez-Martínez, O.; Figueroa-Labastida, M.; Villa-Pulido, A.A.; Sánchez-Fernández, A.; Cué-Sampedro, R.; Gracia-Pinilla, M.A.; Menchaca, J.L. Long-term influence of chitin concentration on the resistance of cement pastes determined by atomic force microscopy. *Phys. Status Solidi A* **2016**, *213*, 3110–3116. [CrossRef]
23. Kaur, S.; Dhillon, G.S. The versatile biopolymer chitosan: Potential sources, evaluation of extraction methods and applications. *Crit. Rev. Microbiol.* **2013**, *40*, 155–175. [CrossRef]
24. Pakizeh, M.; Moradi, A.; Ghassemi, T. Chemical extraction and modification of chitin and chitosan from shrimp shells. *Eur. Polym. J.* **2021**, *159*, 110709. [CrossRef]
25. Hafsa, J.; Smach, M.; Charfeddine, B.; Limem, K.; Majdoub, H.; Rouatbi, S. Antioxidant and antimicrobial properties of chitin and chitosan extracted from *Parapenaeus longirostris* shrimp shell waste. *Ann. Pharm. Fr.* **2016**, *74*, 27–33. [CrossRef]
26. *ASTM C39/C39M*; Standard Test Method for Compressive Strength of Cylindrical Concrete Specimens. ASTM International: West Conshohocken, PA, USA, 2023.
27. *ISO 12571:2021*; Hygrothermal Performance of Building Materials and Products—Determination of Hygroscopic Sorption Properties. International Organization for Standardization: Geneva, Switzerland, 2021.
28. Timmermann, E.O. Multilayer sorption parameters: BET or GAB values? *Colloids Surf. A Physicochem. Eng. Asp.* **2003**, *220*, 235–260. [CrossRef]
29. Prothon, F.; Ahrné, L.l.M. Application of the Guggenheim, Anderson and De Boer model to correlate water activity and moisture content during osmotic dehydration of apples. *J. Food Eng.* **2004**, *613*, 467–470. [CrossRef]
30. Kumari, S.; Rath, P.; Kumar, A.S.H.; Tiwari, T.N. Extraction and Characterization of Chitin and Chitosan from Fishery Waste by Chemical Method. *Environ. Technol. Innov.* **2015**, *3*, 77–85. [CrossRef]
31. Liu, S.; Sun, J.; Yu, L.; Zhang, C.; Bi, J.; Zhu, F.; Qu, M.; Jiang, C.; Yang, Q. Extraction and Characterization of Chitin from the Beetle *Holotrichia parallela* Motschulsky. *Molecules* **2012**, *17*, 4604–4611. [CrossRef]
32. Jabeur, F.; Mechri, S.; Mensi, F.; Gharbi, I.; Ben Naser, Y.; Kriaa, M.; Bejaoui, N.; Bachouche, S.; Badis, A.; Annane, R.; et al. Extraction and Characterization of Chitin, Chitosan, and Protein Hydrolysate from the Invasive Pacific Blue Crab, *Portunus segnis* (Forskål, 1775) Having Potential Biological Activities. *Environ. Sci. Pollut. Res.* **2022**, *29*, 36023–36039. [CrossRef]
33. Hajji, S.; Younes, I.; Ghorbel-Bellaaj, O.; Hajji, R.; Rinaudo, M.; Nasri, M.; Jellouli, K. Structural differences between chitin and chitosan extracted from three different marine sources. *Int. J. Biol. Macromol.* **2014**, *65*, 298–306. [CrossRef]
34. Odeh, A.; Taha, O.S.; Almakhadmeh, M.N.; Al-Rababah, A.; Al-Fakih, A. Comprehensive Review of Polymer-Based Concrete: Properties, Sustainability, and Challenges. *Environ. Sci. Pollut. Res.* **2025**, *32*, 21271–21300. [CrossRef]
35. Andrade, S.M.B.; Ladchumananandasivam, R.; da Rocha, B.G.; Belarmino, D.D.; Galvão, A.O. The Use of Exoskeletons of Shrimp (*Litopenaeus vannamei*) and Crab (*Ucides cordatus*) for the Extraction of Chitosan and Production of Nanomembrane. *Mater. Sci. Appl.* **2012**, *3*, 495–508. [CrossRef]
36. Berodier, E.; Scrivener, K. Understanding the Filler Effect on the Nucleation and Growth of C–S–H. *J. Am. Ceram. Soc.* **2014**, *97*, 3764–3773. [CrossRef]

37. Panesar, D.K.; Zhang, R. Performance comparison of cement replacing materials in concrete: Limestone fillers and supplementary cementing materials—A review. *Constr. Build. Mater.* **2020**, *251*, 118866. [CrossRef]
38. Rahman, M.M.; Muttakin, M.; Pal, A.; Shafiullah, A.Z.; Saha, B.B. A statistical approach to determine optimal models for IUPAC-classified adsorption isotherms. *Energies* **2019**, *12*, 4565. [CrossRef]
39. Baroghel-Bouny, V. Water Vapour Sorption Experiments on Hardened Cementitious Materials. *Cem. Concr. Res.* **2007**, *37*, 414–437. [CrossRef]
40. Abdelhamid, M.B.; Mihoubi, D.; Sghaier, J.; Bellagi, A. Water Sorption Isotherms and Thermodynamic Characteristics of Hardened Cement Paste and Mortar. *Transp. Porous Media* **2016**, *113*, 283–301. [CrossRef]
41. Chalykh, A.E.; Petrova, T.F.; Khasbiullin, R.R.; Ozerin, A.N. Water Sorption on and Water Diffusion in Chitin and Chitosan. *Polym. Sci. Ser. A* **2014**, *56*, 614–622. [CrossRef]
42. Qin, X.; Lin, Y.; Mao, J.; Sun, X.; Xie, Z.; Huang, Q. Research of Water Absorption and Release Mechanism of Superabsorbent Polymer in Cement Paste. *Polymers* **2023**, *15*, 3062. [CrossRef]
43. Synowiecki, J.; Al-Khateeb, N.A. Production, Properties, and Some New Applications of Chitin and Its Derivatives. *Crit. Rev. Food Sci. Nutr.* **2003**, *43*, 145–171. [CrossRef]
44. Mehta, P.K.; Monteiro, P.J.M. *Concrete: Microstructure, Properties, and Materials*, 4th ed.; McGraw-Hill Education: New York, NY, USA, 2014.
45. Scrivener, K.L.; Juilland, P.; Monteiro, P.J.M. Advances in Understanding Hydration of Portland Cement. *Cem. Concr. Res.* **2015**, *78*, 38–56. [CrossRef]
46. Tripathi, B. Effects of Polymers on Cement Hydration and Properties of Concrete: A Review. *ACS Omega* **2024**, *9*, 2014–2021. [CrossRef]
47. Chaabene, K.B.; Dheilly, R.-M.; Promis, G.; Lajili, M. Calcined Crab Shell as a Sustainable Supplementary Cementitious Material in Cement Pastes: Chemical Interaction, Microstructural Evolution, and Mechanical Performance. *Constr. Mater.* **2026**, *6*, 41. [CrossRef]

Disclaimer/Publisher's Note: The statements, opinions and data contained in all publications are solely those of the individual author(s) and contributor(s) and not of MDPI and/or the editor(s). MDPI and/or the editor(s) disclaim responsibility for any injury to people or property resulting from any ideas, methods, instructions or products referred to in the content.